

Vacuum sealing using atomic layer deposition of Al₂O₃ at 250 °C

Seungdo An,^{a)} Naveen K. Gupta,^{a)} and Yogesh B. Gianchandani^{a)}

Center for Wireless Integrated MicroSensing and Systems (WIMS²) and Department of Electrical Engineering and Computer Science, University of Michigan, 1301 Beal Avenue, Ann Arbor, Michigan 48109

(Received 14 May 2013; accepted 21 August 2013; published 5 September 2013)

This paper describes the use of low-temperature atomic layer deposition (ALD) of Al₂O₃, for vacuum seals in wafer-level vacuum packaging and other applications. The conformal coverage provided by ALD Al₂O₃ is shown to seal circular micromachined cavities. The cavities are 0.8 μm in height, 400 μm in diameter, and are capped by porous plasma-enhanced chemical vapor deposited dielectrics that form a membrane. The ALD Al₂O₃ film, of thickness ≈0.2 μm, is deposited at a temperature of 250 °C on this membrane. The retention of vacuum is indicated by the deflection of the membrane. Lifetime tests extending out to 19 months are reported. © 2014 American Vacuum Society. [<http://dx.doi.org/10.1116/1.4820240>]

I. INTRODUCTION

Vacuum sealing is indispensable for many microsystems applications and is commonly used for performance enhancement and device protection. For example, vacuum encapsulation is required for the high quality (high-Q) factor operation for microresonant sensors and actuators, such as gyroscopes,¹ pressure sensors,² and timers.³ Miniaturized analytical instruments, such as gas chromatographs⁴ and mass spectrometers,⁵ together with micropumps⁶ for them, also need pressure-controlled gas flow in microfluidic channels or cavities. In addition, the techniques for achieving and maintaining vacuum seals can be extended to humidity-sensitive electrostatic devices.^{7,8}

For vacuum sealing, wafer-scale encapsulation⁹ is favored over die-level packaging because it offers greater process compatibility, higher throughput, and smaller form factor. In particular, thin-film sealing^{2,10,11} is a natural extension of the surface micromachining process and is preferred to wafer-bonding in many contexts. Typically, an encapsulating membrane is deposited over a patterned sacrificial layer. Holes in this membrane provide access for a gas phase or liquid phase etchant that removes the sacrificial layer. Another thin film is then used to seal the access holes in the membrane. An alternative method is to bond another wafer above the device separated by a spacer layer. Although this circumvents the deposition of a sacrificial layer, it can compromise size and cost, and complicate lead transfer.

Thin-film sealing has been studied for wafer-level vacuum packaging for micromachined resonators.^{1-3,12-17} It has also been explored for sealing microfluidic channels in neural probes.¹⁸ These efforts routinely used common dielectrics, such as silicon oxide or silicon nitride. The films were, in many cases, deposited at temperatures >800 °C, using low-pressure chemical vapor deposition (LPCVD). For lower temperature deposition, plasma-enhanced chemical vapor deposited (PECVD) nitride layers at 450 °C (Ref. 16) and 350 °C (Ref. 19) were used. However, with the decrease

in deposition temperature, the deposited films were as thick as 2.7 and 4.6 μm, respectively. Sputtered AlCu of 1.5 μm thickness, deposited at 350 °C, was also reported for sealing porous poly-SiGe capping membranes.²⁰ Achieving a vacuum seal with a thin film that is deposited at modest temperatures remains a challenging prospect for conventional deposition methods because of the existence of pinholes in deposited films, as well as limitations to the conformality of the deposition.

Atomic layer deposition (ALD) of films is appealing for low temperature sealing. Sequential, self-limiting surface reactions enable the coverage of topographic variations, with film thickness precisely controlled by the number of deposition cycles.^{21,22} The last decade has witnessed increasing efforts to exploit ALD for various sealing purposes that prepare the stage for vacuum sealing. Plasma-enhanced ALD SiO₂ was used to seal mesoporous silica for interlevel dielectrics,²³ and ALD TiO₂ was used to seal nanochannel trenches.²⁴ The deposition temperature of ALD ranges from 25 °C to 300 °C.²¹⁻³² ALD Al₂O₃ was deposited on Kapton, other polymers, and organic light emitting diodes at temperatures as low as 25–125 °C to provide a gas diffusion barrier.^{25-27,30-32} By 2011, it was recognized that ALD layers may be useful for wafer-level vacuum packaging of nano- and microelectromechanical systems.²⁸ Although the deposition of ALD Al₂O₃ on polymer presented major leakage concerns,²⁹ in 2012, the pressure-induced deflection of an ALD Al₂O₃ membrane with a thickness of only 2.8 nm was reported, indicating that the integrity of the film is sufficient to withstand a pressure differential.³³ In addition, it was reported that a thin film barrier of 20–40 nm ALD Al₂O₃ suppresses the water vapor transmission rate to be on the order of 10⁻⁶ gm⁻²day⁻¹,³⁰ which is four orders of magnitude smaller than 100 nm PECVD SiO_x.³⁴ These results suggest that ALD Al₂O₃ could be used potentially for vacuum sealing.^{30,33} In this context, this paper describes an ALD Al₂O₃ low-temperature thin-film vacuum seal for wafer-level vacuum packaging. Section II describes the test structure. Section III details the fabrication process. The test methods, results and discussion are presented in Sec. IV. Concluding remarks are presented in Sec. V.

^{a)}Authors to whom correspondence should be addressed. Electronic addresses: sdan@umich.edu; gnaveen@umich.edu; yogesh@umich.edu

II. TEST STRUCTURE

To determine the vacuum sealing capability of the ALD Al₂O₃ film, a microfabricated test structure is used in this study (Fig. 1). It is composed of a cavity of height $\approx 0.8 \mu\text{m}$ and an encapsulating membrane. The membrane is deflected by the pressure difference between the interior cavity and the ambient atmosphere. Interference patterns, which are caused by the light rays reflected from the upper and lower surfaces of the cavity, present alternating dark and bright fringes as a function of membrane deflection.³⁵ For the deflection to be easily observable, the diameter of the membrane is as large as $400 \mu\text{m}$. The membrane deflections for 160, 460, and 760 Torr are estimated using analytical equations in Ref. 36 (Fig. 2). These estimates take into account the residual stresses of a membrane (which are described in Sec. III). Although the cavity height is $0.8 \mu\text{m}$, deflection is limited by bumps on the lower surface of the cavity (described in Sec. IV). Most fringes are expected to be near the edge; the deflection-limited center region is almost flat. The deflection limit is encountered when the cavity pressure is lower than atmospheric ambient pressure by hundreds of Torr; this provides an indication of the retention of vacuum.

III. FABRICATION PROCESS

The test structure is fabricated by a surface micromachining process, using two masking steps (Fig. 3). The microfabrication process begins with the LPCVD of the first stress-relieved, dielectric oxide-nitride-oxide (ONO-1) stack on a silicon wafer [Fig. 3(a)]. The ONO-1 stack is composed of one nitride layer, thickness $\approx 0.2 \mu\text{m}$ and residual stress $\approx 1.2 \text{ GPa}$, sandwiched by two oxide layers, thickness $\approx 0.5 \mu\text{m}$ and residual stress $\approx -185 \text{ MPa}$. The oxide and nitride layers are deposited at approximately 910 and 800 °C, respectively. This is followed by the deposition of the sacrificial LPCVD polycrystalline silicon (polySi) layer, of thickness $\approx 0.8 \mu\text{m}$, at 585 °C, which is subsequently patterned [Fig. 3(a)]. The cavity height [Fig. 1(a)] is determined by the thickness of the polySi layer. Another LPCVD ONO-2 stack, which is identical to ONO-1, is deposited over the sacrificial polySi layer [Fig. 3(b)]. Slits, $2 \times 10 \mu\text{m}^2$, are patterned in ONO-2 to provide access for the sacrificial etch. The sacrificial polySi layer is etched away by XeF₂ dry gas

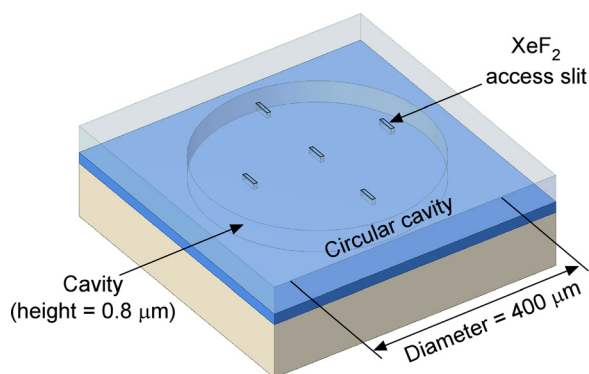


FIG. 1. (Color online) Perspective view of a microfabricated test structure with a circular cavity for testing the ALD Al₂O₃ vacuum seal.

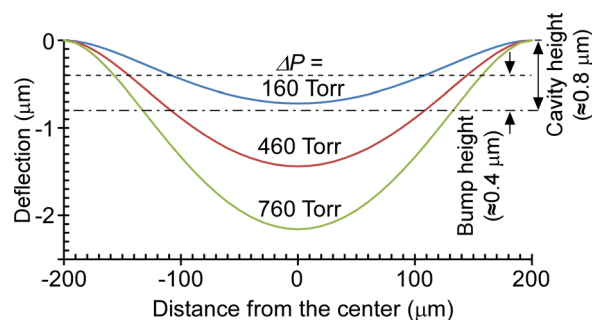


FIG. 2. (Color online) Analytical calculation of the deflection of a circular membrane as a function of pressure difference, ΔP . The pressure difference increases from 160 to 760 Torr by 300 Torr. The membrane deflection is limited by bumps on the cavity floor, the heights of which are indicated by the horizontal dotted line.

[Fig. 3(b)]. Following this, a third stack, ONO-3, is deposited to seal the access slits. The ONO-3 stack, which is deposited by PECVD at 380 °C [Fig. 3(c)], is composed of one nitride layer, thickness $\approx 0.5 \mu\text{m}$ and residual stress $\approx 300 \text{ MPa}$, sandwiched by two oxide layers, thickness $\approx 0.7 \mu\text{m}$ and residual stress $\approx -50 \text{ MPa}$. Even though the PECVD step is performed at $\approx 1 \text{ Torr}$ pressure, the cavities return to atmospheric pressure because the deposited ONO-3 stack is porous. Finally, an ALD Al₂O₃ layer, with thickness $\approx 0.2 \mu\text{m}$ and residual stress $\approx 304 \text{ MPa}$, is deposited at $\approx 300 \text{ mTorr}$ to seal the pores inherent in ONO-3 [as shown in the inset of Fig. 3(c)].

The ALD Al₂O₃ film is deposited using OxfordTM Instruments OpAL.³⁷ Two process options are available: a thermal ALD process performed at 250 °C, which uses water vapor; and another ALD process that uses O₂ plasma. The former is selected because it provides better conformal coverage of topological variations.²¹ For this, the base pressure of the ALD process chamber is $\leq 25 \text{ mTorr}$, and the chamber pressure during growth cycles is maintained at $\approx 300 \text{ mTorr}$ using Ar gas flow. In each cycle for the growth of one atomic layer, the ALD recipe alternates the pulsing of a precursor gas, Al(CH₃)₃, and water vapor, H₂O, to create metal

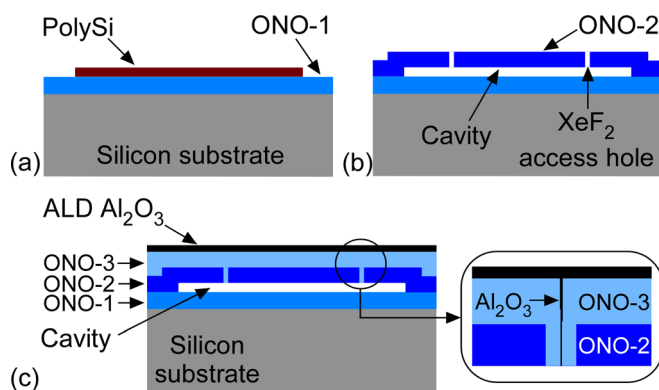
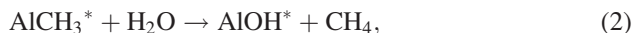


FIG. 3. (Color online) Surface micromachining uses two masking steps. (a) Deposition of LPCVD ONO-1, and deposition and patterning (mask 1) of sacrificial LPCVD polySi. (b) Deposition and patterning (mask 2) of LPCVD ONO-2, and XeF₂ gas dry etching of polySi. (c) Deposition of PECVD ONO-3 and ALD Al₂O₃. The inset in (c) is a magnified view of a sealed access slit.

oxides²¹ (Fig. 4). The overall reaction chemistry in a cycle is described by two half reactions^{21,22}



where the asterisk denotes the surface species. The first step in a cycle is to provide a dose of the precursor to the processing wafer for 20 ms for one layer of Al(CH₃)₂, as shown in Eq. (1) [Fig. 4(a)]. Then, the gaseous by-products or unreacted precursors are purged for 4 s [Fig. 4(a)]. The second step is to provide a dose of the H₂O vapor for 20 ms for the creation of one OH layer on the Al(CH₃)₂ layer, as shown in Eq. (2) [Fig. 4(b)]. Again, the gaseous by-products or unreacted H₂O are purged for 4 s [Fig. 4(b)]. In the first step of the next cycle [Fig. 4(a)], the Al atom within the precursor binds to the O atom by displacing the H atom in the surface adsorbed OH group, as indicated in Eq. (1). Locations where the Al-O attachment did not occur in the first cycle are covered in the second cycle.²¹

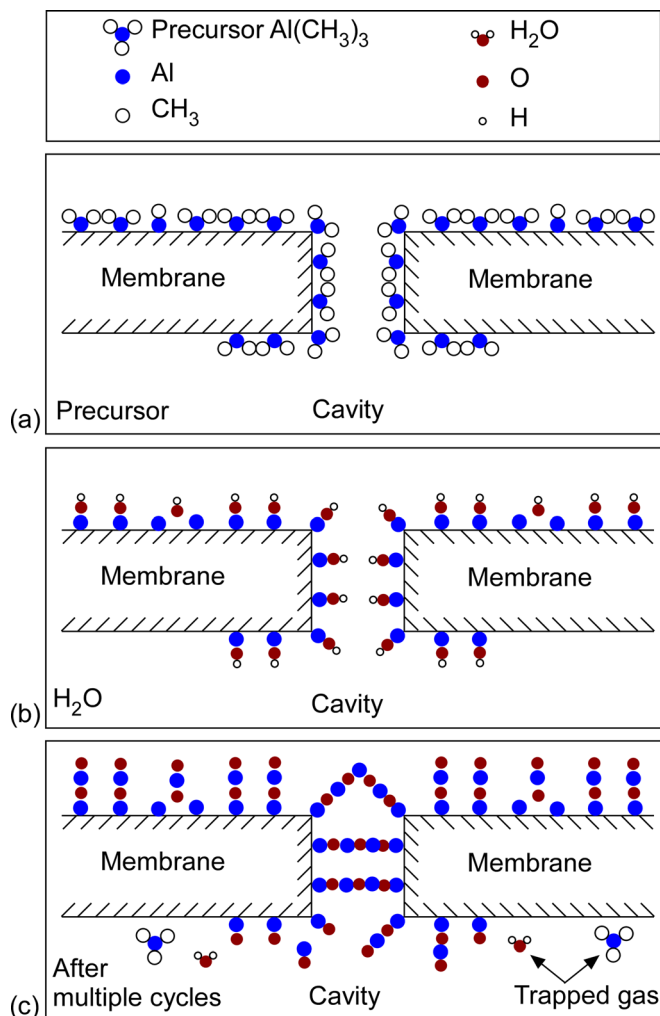


Fig. 4. (Color online) Schematic illustration of a sealing process using ALD Al₂O₃ (Ref. 21). (a) and (b) One cycle of ALD Al₂O₃: (a) dose of precursor Al(CH₃)₃ for 20 ms and purge for 4 s; and (b) dose of H₂O for 20 ms and purge for 4 s. (c) A sealed pore after multiple cycles of ALD Al₂O₃. The figures are not drawn to scale.

By repeating multiple cycles, the pores in PECVD ONO-3 are sealed with multilayered Al₂O₃ [Fig. 4(c)]. However, it is notable that during this process the precursor or H₂O gas molecules might be trapped in the cavity. The total number of cycles for ≈0.2 μm-thickness Al₂O₃ is 1727, in which the growth per cycle (GPC) is ≈0.12 nm; each cycle takes ≈15 s.

IV. TEST RESULTS AND DISCUSSION

As noted previously, optical interference leads to Newton's rings;³⁵ each ring represents a half integer multiple of a laser wavelength, which is 407 nm for the interferogram. When the first bright fringe is assumed to represent no deflection, the first dark fringe corresponds to 1/2 wavelength (≈203.5 nm); the 2nd bright fringe corresponds to 1 wavelength; etc. Although the cavity height is ≈0.8 μm, the membrane ceases further deflection when it touches the ONO-3 bump formed on top of the ONO-1 layer inside the cavity [Fig. 6(a)]; this bump is deposited to a height of ≈0.4 μm through an access slit during the ONO-3 filling process [Fig. 3(c)]. The membrane deflections were analyzed by laser interferogram (Olympus™ LEXT OLS3100) [Fig. 5(a)]. The membrane deflection was also clearly identifiable by visual inspection in an optical microscope with a light source [Fig. 5(b)]. In some cases, the deflected state was further confirmed by intentionally releasing the vacuum (through a nearby perforation); this flattens the membrane and completely removes the fringes.

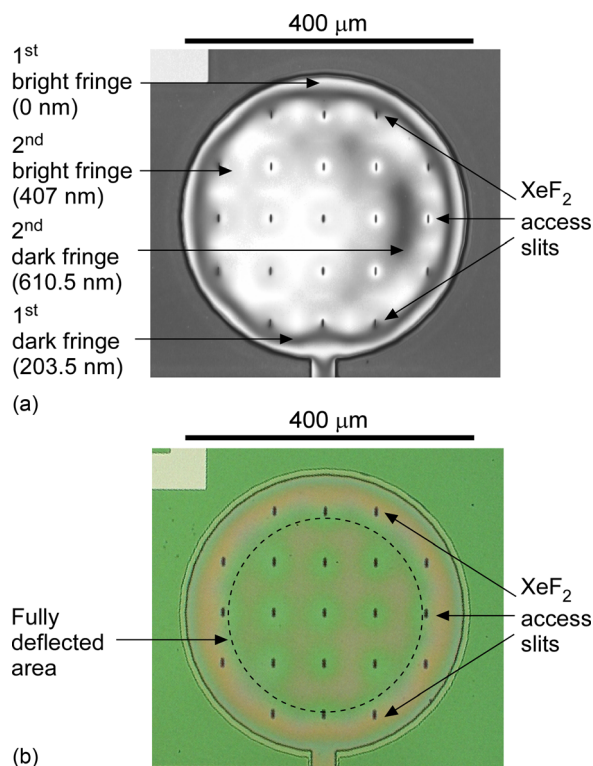
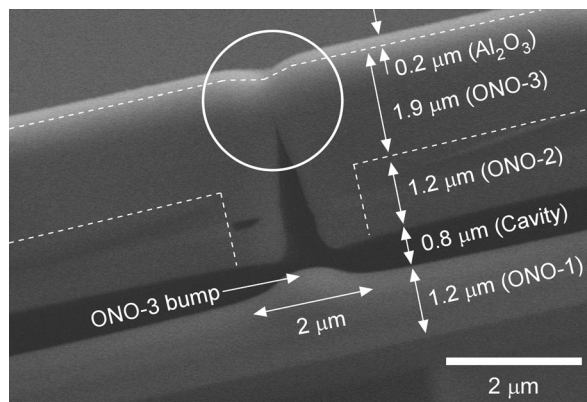


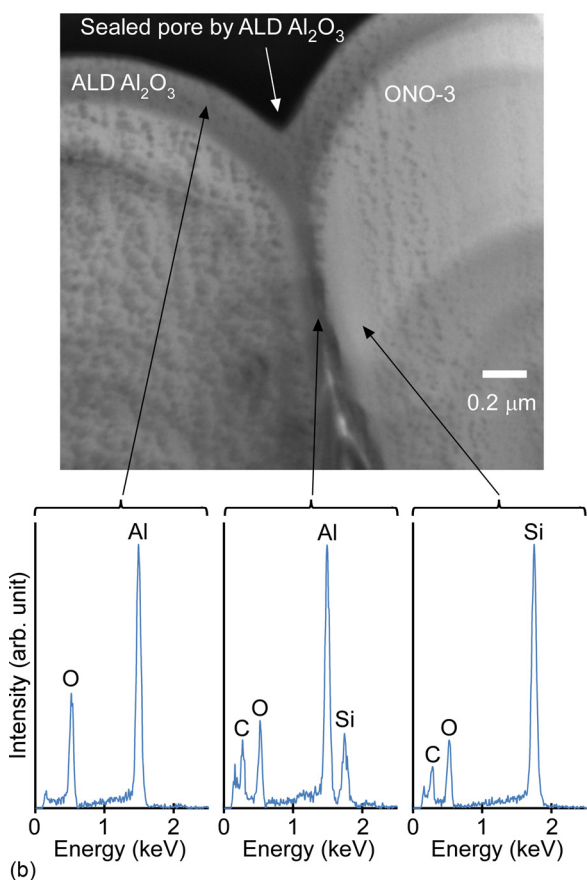
Fig. 5. (Color online) Typical images of deflected circular membranes. (a) A laser interferogram, in which the laser wavelength is 407 nm. (b) An optical microscope image. In (b), the dashed circle indicates the deflected area for which the deflection is limited by the ONO-3 bump inside the cavity. These images are typical of structures examined immediately after fabrication as well as 12 months later.

Structures that were not covered with ALD Al₂O₃ showed no deflection, indicating the cavities were at atmospheric pressure after PECVD dielectric deposition. At the end of the fabrication process, after cavity etch, ALD sealing, and dicing, typically $\approx 69\%$ of the 26 samples in a 100-mm diameter wafer had membranes that were well-formed and appropriately deflected [Fig. 5(b)].

The cross section of a seal was examined by scanning electron microscope (SEM) and transmission electron microscope (TEM), and by energy-dispersive x-ray spectrometry



(a)



(b)

Fig. 6. (Color online) Cross-sectional images of a sealed access slit. (a) SEM image with the expected boundaries between layers. (b) TEM image of the circled area in (a), together with EDS spectra for Al₂O₃, sealed access slit center, and ONO-3. C-related peaks come from TEM sample preparation.

(EDS) (Fig. 6). The XeF₂ access slit is clearly closed by the ONO-3 and ALD Al₂O₃ layers, as shown in the SEM image [Fig. 6(a)]. The boundary of Al₂O₃ and ONO-3 is not evident in the SEM image. However, the boundary is clearly visible under the magnification provided by the TEM image [Fig. 6(b)]. The chemical components in the sealed slit were examined by EDS spectra. The ALD Al₂O₃ spectrum is shown in the first inset of Fig. 6(b), indicating Al- and O-related peaks, without a Si-related peak. The spectrum of the silicon dioxide in ONO-3 is shown in the third inset of Fig. 6(b), indicating Si- and O-related peaks, without an Al-related peak. The spectrum of the central zone, as shown in the second inset of Fig. 6(b), indicates an Al-related peak, together with Si- and O-related peaks. Such Al peaks are also seen in spectra taken on interior surface of the membrane.

Membrane deflections were examined over 19 months while the devices were stored in a clean room. Of the nine membranes that were examined, each one maintained its deflection without any noticeable change (Fig. 7).

The membrane deflection described here is similar to pressure-induced deflection used for bulge tests of deposited films in the past.³³ In contrast to past work, for this paper, the cavity was sealed in vacuum, and the resulting deflection in the ALD Al₂O₃ membrane was maintained over 19 months.

The growth temperature for ALD Al₂O₃ could be potentially decreased below 250 °C to further reduce the thermal budget if necessary. Deposition temperatures less than 100 °C for ALD Al₂O₃ have been reported in Refs. 25, 27, and 29–31. However, it is possible that the quality of the vacuum seal might be compromised. In addition, the image in Fig. 6(b) suggests that the thickness used for this film might be more than necessary.

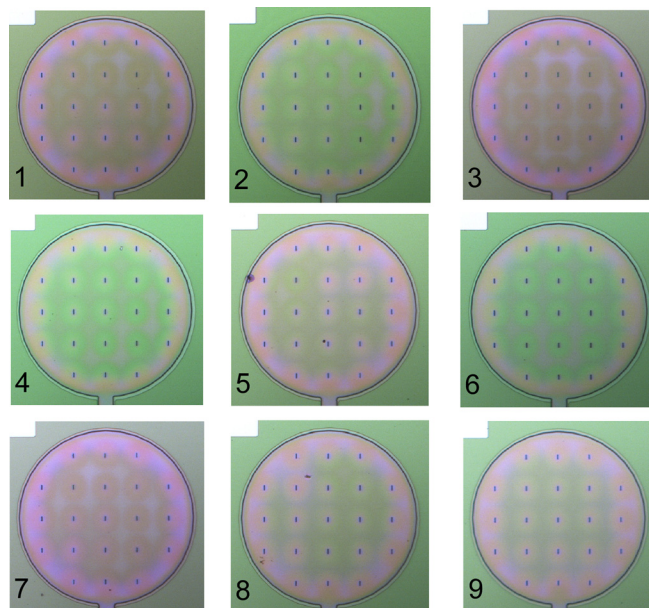


Fig. 7. (Color online) Reliability test of the cavity pressures. Microscope images of nine sealed cavities with circular membranes at 19 months post fabrication are shown.

V. CONCLUSION

Wafer-level vacuum packaging is essential for the performance and protection of many important and widely used microscale devices such as microgyroscopes and pressure sensors. However, achieving and sustaining vacuum with films deposited at modest temperatures has been a persistent challenge. Lower temperatures provide compatibility with the fabrication processes used for the devices, which may generally include CMOS electronics. Thin films of ALD Al₂O₃, which are pin-hole free and highly conformal, are very promising for retaining vacuum seals. The results described in this paper demonstrated that $\approx 0.2 \mu\text{m}$ -thick ALD Al₂O₃ at 250 °C is sufficient to provide a seal to vacuum cavities that are $\approx 0.8 \mu\text{m}$ in height, 400 μm in diameter, and are capped with PECVD dielectrics that are otherwise porous. The sealed cavities retained vacuum for a period exceeding 19 months.

Future efforts can be directed at further reducing the thermal budget of the process. Additional efforts may be directed at using embedded sensors for quantitative analysis of cavity pressures.

ACKNOWLEDGMENTS

S.A. acknowledges partial support by a fellowship from the Electrical Engineering and Computer Science Department at the University of Michigan, Ann Arbor. This study was supported in part by the Microsystems Technology Office of the Defense Advanced Research Projects Agency High-Vacuum program (DARPA Contract #W31P4Q-09-1-0011). Facilities used for this research included the Lurie Nanofabrication Facility (LNF) operated by the Solid-State Electronics Laboratory (SSEL) and the University of Michigan.

- ¹K. Liu, W. Zhang, W. Chen, K. Li, F. Dai, F. Cui, X. Wu, G. Ma, and Q. Xiao, *J. Micromech. Microeng.* **19**, 113001 (2009).
- ²K. Ikeda, H. Kuwayama, T. Kobayashi, T. Watanabe, T. Nishikawa, T. Yoshida, and K. Harada, *Sens. Actuator A* **23**, 1007 (1990).
- ³J. T. M. van Beek and R. Puers, *J. Micromech. Microeng.* **22**, 013001 (2012).
- ⁴J. Liu, N. K. Gupta, K. D. Wise, Y. B. Gianchandani, and X. Fan, *Lab Chip* **11**, 3487 (2011).
- ⁵J. P. Hauschild, E. Wapelhorst, and J. Muller, *Int. J. Mass Spectrom.* **264**, 53 (2007).
- ⁶H. Kim, K. Najafi, and L. Bernal, *Comprehensive Microsystems*, edited by Y. B. Gianchandani, O. Tabata, and H. Zappe (Elsevier Publishers, 2008), Vol. 2, pp. 273–299.

- ⁷P. F. van Kessel, L. J. Hornbeck, R. E. Meier, and M. R. Douglass, *Proc. IEEE* **86**, 1687 (1998).
- ⁸M. C. Wu, O. Solgaard, and J. E. Ford, *J. Lightwave Technol.* **24**, 4433 (2006).
- ⁹M. Esashi, *J. Micromech. Microeng.* **18**, 073001 (2008).
- ¹⁰H. Guckel and D. W. Burns, in *IEEE International Electron Devices Meeting*, San Francisco, CA (1984), pp. 223–225.
- ¹¹H. Guckel and D. W. Burns, U.S. patent 4,853,669 (1 August 1989).
- ¹²L. Lin, R. T. Howe, and A. P. Pisano, *J. Microelectromech. Syst.* **7**, 286 (1998).
- ¹³T. Tsuchiya, Y. Kageyama, H. Funabashi, and J. Sakata, *Sens. Actuator A* **90**, 49 (2001).
- ¹⁴R. N. Candler *et al.*, *J. Microelectromech. Syst.* **15**, 1446 (2006).
- ¹⁵M. Chiao and L. Lin, *J. Microelectromech. Syst.* **15**, 515 (2006).
- ¹⁶Q. Li, J. F. L. Goosen, J. T. M. van Beek, F. van Keulen, K. L. Phan, and G. Q. Zhang, *Microelectron. Reliab.* **48**, 1557 (2008).
- ¹⁷S. Yoneoka, C. S. Roper, R. N. Candler, S. A. Chandorkar, A. B. Graham, J. Provine, R. Maboudian, R. T. Howe, and T. W. Kenny, *J. Microelectromech. Syst.* **19**, 357 (2010).
- ¹⁸K. D. Wise, A. M. Sodagar, Y. Yao, M. N. Gulari, G. E. Perlin, and K. Najafi, *Proc. IEEE* **96**, 1184 (2008).
- ¹⁹C. Liu and Y.-C. Tai, *J. Microelectromech. Syst.* **8**, 135 (1999).
- ²⁰B. Guo *et al.*, *J. Microelectromech. Syst.* **21**, 110 (2012).
- ²¹R. L. Puurunen, *J. Appl. Phys.* **97**, 121301 (2005).
- ²²S. M. George, *Chem. Rev.* **110**, 111 (2010).
- ²³Y.-B. Jiang, N. Liu, H. Gerung, J. L. Cecchi, and C. J. Brinker, *J. Am. Chem. Soc.* **128**, 11018 (2006).
- ²⁴S.-W. Nam, M.-H. Lee, S.-H. Lee, D.-J. Lee, S. M. Rosnagel, and K.-B. Kim, *Nano Lett.* **10**, 3324 (2010).
- ²⁵C. A. Wilson, R. K. Grubbs, and S. M. George, *Chem. Mater.* **17**, 5625 (2005).
- ²⁶P. F. Carcia, R. S. McLean, M. D. Groner, A. A. Dameron, and S. M. George, *J. Appl. Phys.* **106**, 023533 (2009).
- ²⁷C. Lin, Y. Zhang, A. Abdulagatov, R. Yang, S. George, and Y. C. Lee, in *IEEE International Conference on Micro Electro Mechanical Systems*, Wanchai, Hong Kong (2010), pp. 528–531.
- ²⁸Y. C. Lee, *Proc. SPIE* **7928**, 792802 (2011).
- ²⁹Y. Zhang, Ph.D. dissertation (University of Colorado, Boulder, 2011).
- ³⁰W. Keuning, P. van de Weijer, H. Lifka, W. M. M. Kessels, and M. Creatore, *J. Vac. Sci. Technol. A* **30**, 01A131 (2012).
- ³¹E. Dickey and W. A. Barrow, *J. Vac. Sci. Technol. A* **30**, 021502 (2012).
- ³²P. F. Carcia, R. S. McLean, Z. G. Li, M. H. Reilly, and W. J. Marshall, *J. Vac. Sci. Technol. A* **30**, 041515 (2012).
- ³³L. Wang, J. J. Travis, A. S. Cavanagh, X. Liu, S. P. Koenig, P. Y. Huang, S. M. George, and J. S. Bunch, *Nano Lett.* **12**, 3706 (2012).
- ³⁴A. M. Coclite, F. D. Luca, and K. K. Gleason, *J. Vac. Sci. Technol. A* **30**, 061502 (2012).
- ³⁵A. Al-Azzawi, *Photonics: Principles and Practices* (CRC, Boca Raton, FL, 2006), 336 pp.
- ³⁶Y. B. Gianchandani, C. G. Wilson, and J.-S. Park, *The MEMS Handbook*, 2nd ed., edited by M. Gad-el-Hak (CRC, Boca Raton, FL, 2006), Chap. 3.
- ³⁷See: <http://www.oxford-instruments.com/products/etching-deposition-and-growth/plasma-etch-deposition/atomic-layer-deposition> for Oxford ALD website (March 2013).